

MADPH-96-957

TTP96-38

hep-ph/yymmxxx

August 1996

# Forward Jet Production at HERA in the Low $x$ Regime in Next-to-Leading Order

Erwin Mirkes<sup>1</sup> and Dieter Zeppenfeld<sup>2</sup><sup>1</sup>*Institut für Theoretische Teilchenphysik, Universität Karlsruhe,**D-76128 Karlsruhe, Germany*<sup>2</sup>*Department of Physics, University of Wisconsin, Madison, WI 53706, USA*

## Abstract

The production of forward jets of transverse momentum  $p_T(j) \approx Q$  and large momentum fraction  $x_{jet} \gg x$  probes the onset of BFKL dynamics at HERA. A full  $\mathcal{O}(\alpha_s^2)$  calculation of the inclusive forward jet cross section is presented and compared to the expected BFKL cross section. The kinematical region populated by these events and the scale dependence of the fixed order perturbative QCD cross sections are discussed.

Deep-inelastic scattering (DIS) at HERA provides for an ideal place to probe strong interaction dynamics at small Bjorken  $x$ . One focus of interest has been the rise of the structure function  $F_2(x, Q^2)$  [1] for large  $1/x$ . One would like to identify the power law growth,  $1/x^{\alpha_p-1}$ , as predicted by the Balitsky-Fadin-Kuraev-Lipatov (BFKL) [2] evolution equation. This evolution equation resums all leading  $\alpha_s \ln 1/x$  terms, as opposed to the more standard Dokshitzer-Gribov-Lipatov-Altarelli-Parisi (DGLAP) equation [3] which resums all leading  $\alpha_s \ln Q^2$  terms. Unfortunately, the measurement of  $F_2$  in the HERA range is probably too inclusive to discriminate between BFKL and the conventional DGLAP dynamics [4].

A more sensitive test of BFKL dynamics at small  $x$  is expected from deep inelastic scattering with a measured forward jet (in the proton direction) and  $p_T^2(j) \approx Q^2$  [5]. The idea is to study DIS events which contain an identified jet of longitudinal momentum fraction  $x_{jet} = p_z(jet)/E_{proton}$  which is large compared to Bjorken  $x$ .

One of the dominant Feynman graphs responsible for the parton evolution is shown in Fig. 1 for the particular case of a gluon initiated process. The  $x_i$  denote the momentum fractions (relative to the incoming proton) of the incident virtual partons and  $p_{Ti}$  is the transverse momentum of emitted parton  $i$ . In the axial gauge, such “ladder-type” diagrams with strong ordering in transverse momenta,  $Q^2 \approx p_{Tn}^2 \gg \dots \gg p_T(j)^2$  but only soft ordering for the longitudinal fraction  $x_1 > x_2 > \dots > x_n \approx x$  are the source of the leading  $\log Q^2$  contribution. In the BFKL approximation transverse momenta are no longer ordered along the ladder while there is a strong ordering in the fractional momentum  $x_n \ll x_{n-1} \ll \dots \ll x_1 \approx x_{jet}$ . When tagging a forward jet with  $p_T(j) \approx Q$  this leaves little room for DGLAP evolution while the condition  $x_{jet} \gg x$  leaves BFKL evolution active. This leads to an enhancement of the forward jet production cross section proportional to  $(x_{jet}/x)^{\alpha_P-1}$  over the DGLAP expectation.

Fig. 1 shows that the gluon ladders responsible for BFKL evolution first appear at  $\mathcal{O}(\alpha_s^3)$ , i.e. for processes with at least four scattered partons in the final state. A conventional fixed order QCD calculation up to  $\mathcal{O}(\alpha_s^2)$  contains no trace of BFKL dynamics and must be considered a background for its detection; one must search for an enhancement in the

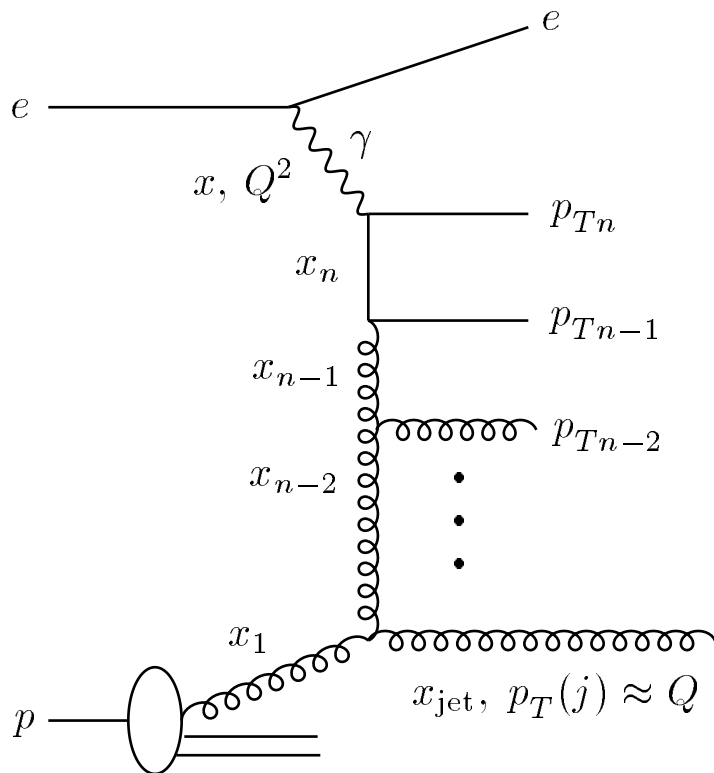


FIG. 1. Gluon ladder diagram contributing to jet production in DIS. The position and kinematics of the parton which can give rise to the forward jet is indicated.

forward jet production cross section above the expectation for two- and three-parton final states.

In this Letter we perform a full next-to-leading order (NLO) analysis of this “fixed order” background. Such an analysis has become possible with the implementation of QCD radiative corrections to dijet production in DIS in a fully flexible Monte Carlo program, MEPJET [6]. The program integrates the cross sections for two-parton and three-parton final states numerically and at each phase space point the four-momenta of all final state particles are available. This allows to implement arbitrary experimental cuts and arbitrary jet definition schemes. Collinear and infrared divergences in the naive three-parton cross section are removed by slicing the three parton phase space into a hard region, where all

two-parton invariant masses squared are above a technical cutoff parameter  $s_{min}$ , and the remaining soft and/or collinear cross section is added to the virtual contributions, yielding a finite two-parton cross section after splitting off initial state collinear divergences into universal crossing functions [7].  $s_{min}$ -independence of the resulting cross section [6] is a powerful test of the integration program. For the forward jet phase space region to be discussed below we have verified this independence to better than 1%, which is the statistical accuracy of our Monte Carlo runs.

Numerical results below will be presented both for leading order (LO) and NLO simulations. The LO 1-jet and 2-jet results employ the LO parton distributions of Glück, Reya and Vogt [8,9] together with the one-loop formula for the strong coupling constant. At  $\mathcal{O}(\alpha_s^2)$  all cross sections are determined using the NLO GRV parton distribution functions  $f(x_1, \mu_F^2)$  and the two loop formula for  $\alpha_s(\mu_R^2)$ . With this procedure the 2-jet inclusive rate at NLO is simply given as the sum of the NLO 2-jet and the LO 3-jet exclusive cross sections. The value of  $\alpha_s$  is matched at the thresholds  $\mu_R = m_q$  and the number of flavors is fixed to  $n_f = 5$  throughout, *i.e.* gluons are allowed to split into five flavors of massless quarks.

Unless otherwise stated, both the renormalization and the factorization scales are tied to the sum of parton  $k_T$ 's in the Breit frame,

$$\mu_R = \mu_F = \frac{1}{2} \sum_i k_T^B(i), \quad (1)$$

where  $(k_T^B(i))^2 = 2E_i^2(1 - \cos\theta_{ip})$ . Here  $\theta_{ip}$  is the angle between the parton and proton directions in the Breit frame.  $\sum_i k_T^B(i)$  constitutes a natural scale for jet production in DIS [10] because it interpolates between  $Q$ , in the naive parton model limit, and the sum of jet transverse momenta, when  $Q$  becomes negligible.

We are interested in events with a forward jet with  $p_T(j) \approx Q$  and  $x_{jet} \gg x$  and impose kinematical cuts which closely model the H1 selection [11] of such events. Jets are defined in the cone scheme (in the laboratory frame) with  $\Delta R = 1$  and  $|\eta| < 3.5$ . Here  $\eta = -\ln \tan(\theta/2)$  denotes the pseudo-rapidity of a jet. Unless noted otherwise, all jets must have transverse momenta of at least 4 GeV in both the laboratory and the Breit frames.

Events are selected which contain a forward jet (denoted “ $j$ ”) in the pseudo-rapidity range  $1.735 < \eta(j) < 2.9$  (corresponding to  $6.3^\circ < \theta(j) < 20^\circ$ ) and with transverse momentum  $p_T^{lab}(j) > 5$  GeV. This jet must satisfy

$$x_{jet} = p_z(j)/E_p > 0.05 , \quad (2)$$

$$0.5 < p_T^2(j)/Q^2 < 4 , \quad (3)$$

in the laboratory frame. The condition  $x_{jet} \gg x$  is satisfied by requiring

$$x < 0.004 . \quad (4)$$

Additional selection cuts are  $Q^2 > 8$  GeV<sup>2</sup>,  $0.1 < y < 1$ , an energy cut of  $E(l') > 11$  GeV on the scattered lepton, and a cut on its pseudo-rapidity of  $-2.868 < \eta(l') < -1.735$  (corresponding to  $160^\circ < \theta(l') < 173.5^\circ$ ). The energies of the incoming electron and proton are set to 27.5 GeV and 820 GeV, respectively.

Numerical results for the multi-jet cross sections are shown in Table I. Without the requirement of a forward jet, the cross sections show the typical decrease with increasing jet multiplicity which is expected in a well-behaved QCD calculation. The 3-jet cross section in the last column constitutes only about 10% of the 2-jet cross section and both rates are sizable. The requirement of a forward jet with large longitudinal momentum fraction ( $x_{jet} > 0.05$ ) and restricted transverse momentum ( $0.5 < p_T^2(j)/Q^2 < 4$ ) severely restricts the available phase space. In particular one finds that the 1-jet cross section vanishes at LO, due to the contradicting  $x < 0.004$  and  $x_{jet} > 0.05$  requirements: this forward jet kinematics is impossible for one single massless parton in the final state.

Suppose now that we had performed a full  $\mathcal{O}(\alpha_s^2)$  calculation of the DIS cross section, which would contain 3-parton final states at tree level, 1-loop corrections to 2-parton final states and 2-loop corrections to 1-parton final states. These 2-loop contributions would vanish identically, once  $x \ll x_{jet}$  is imposed. The remaining 2-parton and 3-parton differential cross sections, however, and the cancelation of divergences between them, would be the same as those entering a calculation of 2-jet inclusive rates. These elements are

TABLE I. Cross sections for  $n$ -jet events in DIS at HERA at order  $\alpha_s^0$ ,  $\alpha_s$ , and  $\alpha_s^2$ . The jet multiplicity includes the forward jet which, when required, must satisfy  $p_T(j) > 5$  GeV and the cuts of Eq. (2,3). The transverse momenta of additional (non-forward) jets must only exceed cuts of 4 GeV (first and third column). This requirement is replaced by the condition  $k_T^B > 4$  GeV in the second column. No  $p_T^B$  cut is imposed in the 1-jet case at  $\mathcal{O}(\alpha_s^0)$  and the factorization scale is fixed to  $Q$ . See text for further details.

	with forward jet		without forward jet
	$p_T^B, p_T^{lab} > 4$ GeV	$k_T^B > 4$ GeV	$p_T^B, p_T^{lab} > 4$ GeV
$\mathcal{O}(\alpha_s^0)$ : 1 jet	0 pb	0 pb	8630 pb
$\mathcal{O}(\alpha_s)$ : 2 jet	18.9 pb	22.4 pb	2120 pb
$\mathcal{O}(\alpha_s^2)$ : 1 jet inclusive	100 pb	100 pb	
2 jet inclusive	83.8 pb	98.3 pb	2400 pb
2 jet exclusive	69.0 pb	66.8 pb	2190 pb
3 jet	14.8 pb	31.5 pb	210 pb

already implemented in the MEPJET program which, therefore, can be used to determine the inclusive forward jet cross section within the cuts of Eqs. (2-4). At  $\mathcal{O}(\alpha_s^2)$  this cross section is obtained from the cross section for 2-jet inclusive events by integrating over the full phase space of the additional jets, without any cuts on their transverse momenta or pseudo-rapidities. Numerical results are shown in the third row of Table I.

The table exhibits some other remarkable features of forward jet events: the NLO 2-jet inclusive cross section exceeds the LO 2-jet cross section by more than a factor four and the 3-jet rate at  $\mathcal{O}(\alpha_s^2)$  is about as large as the 2-jet rate at  $\mathcal{O}(\alpha_s)$ . These characteristics can be understood in terms of the kinematics of forward jet events. Kinematics puts severe constraints on the “recoil system”, the part of the final state in the  $\gamma$ -parton collision of Fig. 1 which is left after taking out the forward jet. For  $x \ll x_{jet}$ , a high invariant mass

hadronic system must be produced by the photon-parton collision. For small scattering angle but large energy,  $E(j)$ , of the forward jet this condition translates into

$$M^2 + 2E(j)m_T e^{-y} \approx \hat{s}_{\gamma,parton} \gtrsim Q^2 \left( \frac{x_{jet}}{x} - 1 \right) \gg Q^2. \quad (5)$$

Here  $m_T = \sqrt{M^2 + p_T^2}$  and  $y$  are the transverse mass and rapidity of the partonic recoil system. Eq. (5) implies that  $m_T$  must be large, the more so the larger the ratio  $x_{jet}/x$ . On the other hand, the transverse momentum,  $p_T$ , of the recoil system is fixed by momentum conservation,  $p_T = |\mathbf{q}_T + \mathbf{p}_T(j)|$ , and the cross section is largest when the transverse momenta of both the virtual photon,  $q_T$ , and of the forward jet are small. Thus, a large recoil transverse mass is most easily achieved by two or more partons which create a subsystem of large invariant mass,  $M$ , and some of these partons will manifest themselves as fairly hard hadronic jets.

This fact is demonstrated in Fig. 2 where the transverse momentum and the pseudo-rapidity distributions of the recoil jet with the highest  $p_T^{lab}$  are shown, subject only to a nominal requirement of  $p_T^{lab}, p_T^B > 1$  GeV. Almost all forward jet events contain at least one second jet, with  $p_T^{lab} \gtrsim 4$  GeV, which typically falls into the central part of the detector.

In the usual cone scheme final state collinear singularities are regulated by the  $\Delta R$  separation cut while infrared singularities and initial state collinear emission are regulated by the  $p_T$  cut. In  $\gamma^*p$  collisions the photon virtuality,  $Q^2$ , eliminates any collinear singularities for initial state emission in the electron direction and therefore a large  $k_T$  is as good a criterion to define a cluster of hadrons as a jet as its  $p_T$ . The dashed line in Fig. 2(a) shows the  $k_T$  distribution in the Breit frame of the recoil jet candidate with the largest  $k_T^B$ . Basically all forward jet events in this NLO analysis possess a recoil “jet” with  $k_T^B > 4$  GeV and would thus be classified as 2-jet inclusive events in a variant of the cone scheme where the  $p_T > 4$  GeV condition is replaced by a  $k_T^B > 4$  GeV cut. This observation makes intuitively clear why we are able to calculate the 1-jet inclusive forward jet cross section with a program which calculates the dijet inclusive cross section at NLO: there exists a jet definition scheme in which all forward jet events contain at least one additional hard jet.

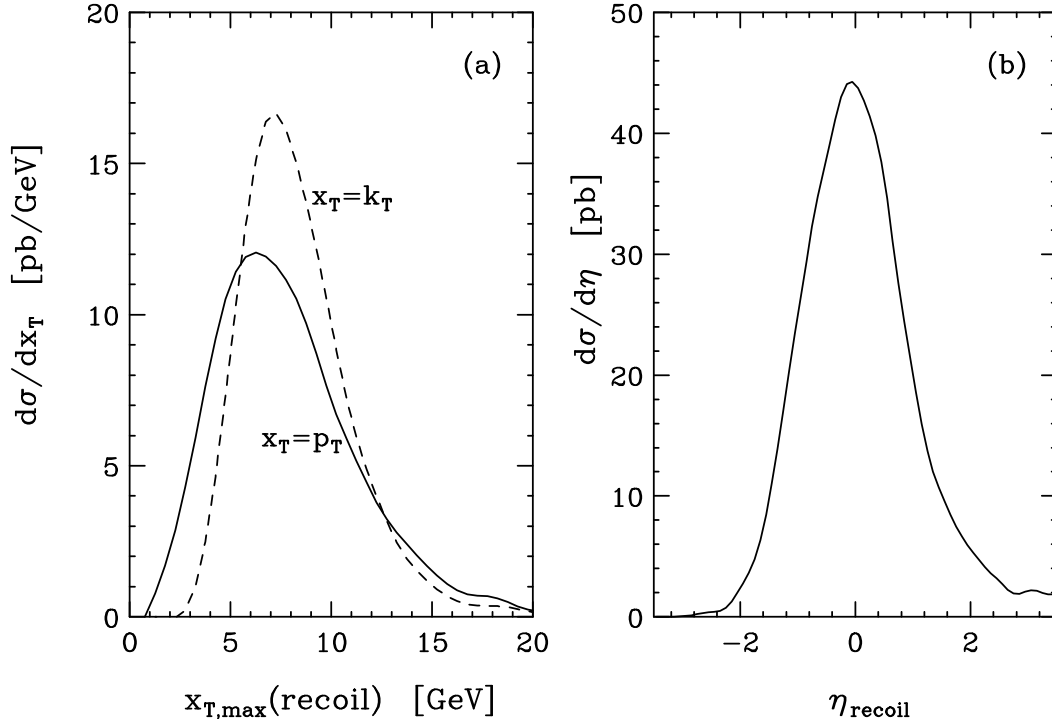


FIG. 2. Characteristics of the highest transverse momentum “jet” in the recoil system, i.e. excluding the forward jet. Distributions shown are (a)  $d\sigma/dp_T$  in the lab frame (solid line) and  $d\sigma/dk_T$  in the Breit frame (dashed line) and (b) the jets pseudo-rapidity distribution in the laboratory frame. All distributions are calculated at order  $\alpha_s^2$ . Jet transverse momentum cuts have been relaxed to  $p_T^{lab}, p_T^B > 1$  GeV.

How reliable is the determination of the forward jet cross section at NLO? The importance of higher order corrections can be estimated by studying the dependence of the cross section on the choice of factorization and renormalization scales,  $\mu_F$  and  $\mu_R$ . Our standard choice is  $\mu_R^2 = \mu_F^2 = \frac{1}{4} \left( \sum_i k_T^B(i) \right)^2$ . In Fig. 3 we investigate variations of the 2-jet inclusive cross section when changing this scale by a factor,  $\xi$ , (solid lines)

$$\mu_R^2 = \mu_F^2 = \xi \frac{1}{4} \left( \sum_i k_T^B(i) \right)^2, \quad (6)$$

and we also consider renormalization and factorization scales which are proportional to the photon virtuality,  $Q^2$ , (dashed lines)

$$\mu_R^2 = \mu_F^2 = \xi Q^2. \quad (7)$$



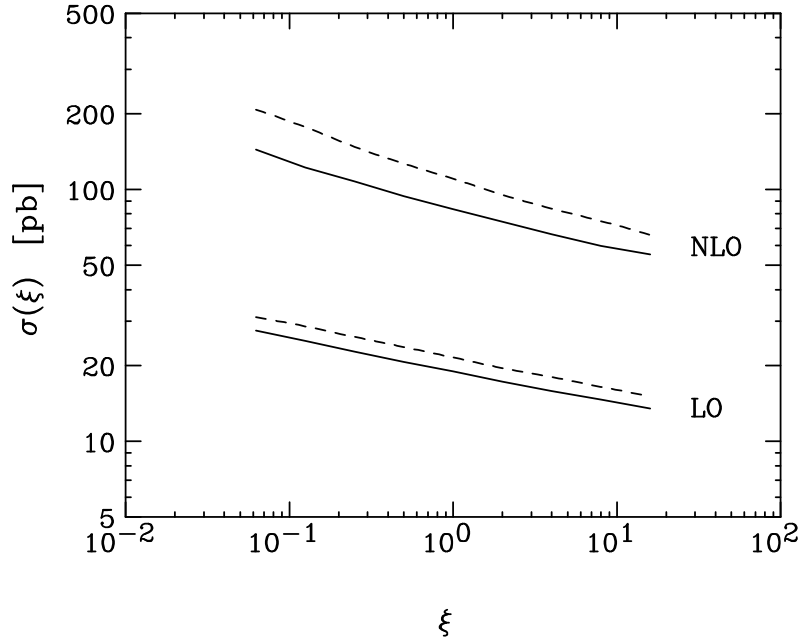


FIG. 3. Scale dependence of the 2-jet inclusive cross section with a forward jet satisfying  $x_j > 0.05$  and  $p_{Tj} > 5$  GeV in the lab frame (see text for additional cuts). Results are shown for  $\mu_R^2 = \mu_F^2 = \xi Q^2$  (dashed lines) and  $\mu_R^2 = \mu_F^2 = \xi(0.5 \sum k_T)^2$  (solid lines), at LO (lower curves) and at NLO (upper curves).

Two striking features of the forward jet cross section become apparent in this comparison. The large effective  $K$ -factor,  $K \approx 5$ , was already noted in Table I. In addition one finds that the scale dependence is at least as strong at NLO as at LO. Both features are closely related. The smallness of the LO 2-jet compared to the NLO 2-jet inclusive cross section means that at least three final state partons are required to access the relevant part of the phase space. This three-parton cross section, however, has only been calculated at tree level and is subject to the typical scale uncertainties of a tree level calculation. Thus, even though we have performed a full  $\mathcal{O}(\alpha_s^2)$  calculation of the forward jet cross section at HERA, including all virtual effects, our calculation effectively only gives a LO estimate of this cross section and large corrections may be expected from higher order effects, like the gluon ladders in Fig. 1.

The size of these corrections may be estimated by comparing to BFKL calculations or to existing experimental results. The H1 Collaboration has published such a measurement which was made during the 1993 HERA run with incident electron and proton energies of

$E_e = 26.7$  GeV and  $E_p = 820$  GeV [12]. The acceptance cuts used for this measurement differed somewhat from the ones described before. Because of the lower luminosity in this early HERA run the  $x_{jet}$  cut on the forward jet was lowered to 0.025 and defined in terms of the jet energy as opposed to the longitudinal momentum of the jet in the proton direction,

$$x_{jet} = E(j)/E_p > 0.025 , \quad (8)$$

and the pseudo-rapidity range of the forward jet was chosen slightly larger,  $1.735 < \eta(j) < 2.949$  (corresponding to  $6^\circ < \theta(j) < 20^\circ$ ). Scattered electrons were selected with an energy of  $E(l') > 12$  GeV and in the pseudo-rapidity range  $-2.794 < \eta(l') < -1.735$  (corresponding to  $160^\circ < \theta(l') < 173^\circ$ ). Finally the Bjorken- $x$  and  $Q^2$  ranges were chosen as  $0.0002 < x < 0.002$  and  $5 \text{ GeV}^2 < Q^2 < 100 \text{ GeV}^2$ . Within these cuts H1 has measured cross sections of  $709 \pm 42 \pm 166$  pb for  $0.0002 < x < 0.001$  and  $475 \pm 39 \pm 110$  pb for  $0.001 < x < 0.002$ . These two data points, normalized to bin sizes of 0.0002, are shown as diamonds with error bars in Fig. 4. Also included (dashed histogram) is a recent calculation of the BFKL cross section [13].

As shown before, the MEPJET program allows to calculate the full 1-jet inclusive forward jet cross section<sup>1</sup> for  $x \ll x_{jet}$ . The LO result is shown as the dash-dotted histogram in Fig. 4 and the NLO result is shown as the solid histogram. The shaded area corresponds to a scale variation

$$\mu_R^2 = \mu_F^2 = \xi \frac{1}{4} \left( \sum_i k_T^B(i) \right)^2 , \quad (9)$$

from  $\xi = 0.1$  to  $\xi = 10$ , and indicates a range of “reasonable” expectations for the forward jet cross section at  $\mathcal{O}(\alpha_s^2)$ .

While the BFKL results [13] agree well with the H1 data, the fixed order perturbative QCD calculations clearly fall well below the measured cross section, even when accounting

---

<sup>1</sup>We have checked that also for the kinematical region considered now almost all forward jet events contain at least one second jet with  $p_T^{lab} > 4$  GeV and  $k_T^B > 4$  GeV.

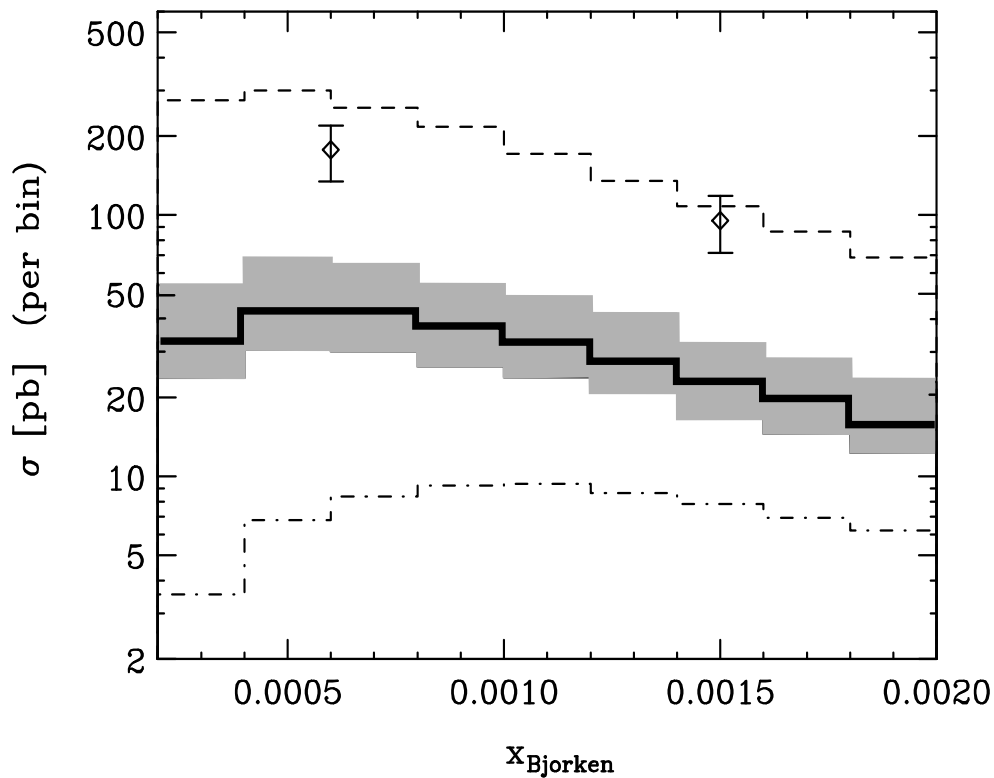


FIG. 4. Forward jet cross section at HERA as a function of Bjorken  $x$  within the H1 acceptance cuts [12] (see text). The solid (dash-dotted) histogram gives the NLO (LO) MEPJET result for the scale choice  $\mu_R^2 = \mu_F^2 = \xi(0.5 \sum k_T)^2$  with  $\xi = 1$ . The shaded area shows the uncertainty of the NLO prediction, corresponding to a variation of  $\xi$  between 0.1 and 10. The BFKL result of Bartels et al. [13] is shown as the dashed histogram. The two data points with error bars correspond to the H1 measurement [12].

for variations of the factorization and renormalization scales. The measured cross section is a factor 4 above the NLO expectation. The shape of the NLO prediction, on the other hand, is perfectly compatible with the H1 results, and not very different from the BFKL curve in Fig. 4. At LO a marked shape difference is still observed, which can be traced directly to the kinematical arguments given before: according to Eq. (5) the transverse mass of the recoil system must increase proportional to  $x_{jet}/x$  and this requires increased transverse momentum of the forward jet at LO. Thus, at LO, the expected cross section falls rapidly at small  $x$ , an effect which is avoided when additional partons are available in the final state

to balance the overall transverse momentum.

We conclude that the existing H1 data show evidence for BFKL dynamics in forward jet events via an enhancement in the observed forward jet cross section above NLO expectations. The variation of the cross section with  $x$ , on the other hand, is perfectly compatible with either BFKL dynamics or NLO QCD. Since MEPJET provides a full NLO prediction of the 1-jet inclusive forward jet cross section for arbitrary cuts and jet definition schemes, more decisive shape tests may be possible as additional data become available.

### ACKNOWLEDGMENTS

This research was supported by the University of Wisconsin Research Committee with funds granted by the Wisconsin Alumni Research Foundation and by the U. S. Department of Energy under Grant No. DE-FG02-95ER40896. The work of E. M. was supported in part by DFG Contract Ku 502/5-1.

## REFERENCES

- [1] H1 Collaboration, Phys. Lett. **B356** (1995) 118;  
ZEUS Collaboration, Z. Phys. **C69** (1996) 607.
- [2] E.A. Kuraev, L.N. Lipatov and V.S. Fadin, Sov. Phys. **JETP** **45** (1977) 199;  
Y.Y. Balitsky and L.N. Lipatov, Sov. J. Nucl. Phys. **28** (1978) 282.
- [3] G. Altarelli and G. Parisi, Nucl. Phys. **126** (1977) 297;  
V.N. Gribov and L.N. Lipatov, Sov. J. Nucl. Phys. **15** (1972) 438 and 675;  
Yu. L. Dokshitzer, Sov. Phys. **JETP** **46** (1977) 641.
- [4] A.D. Martin, Acta Physica Polonica **B27** (1996) 1287;  
A. De Roeck, Acta Physica Polonica **B27** (1996) 1175.
- [5] A.H. Mueller, Nucl. Phys. B (Proc. Suppl.) **18C** (1990) 125; J. Phys. **G17** (1991) 1443;  
J. Kwiecinski, A.D. Martin and P.J. Sutton, Phys. Rev. **D46** (1992) 921;  
W.K. Tang, Phys. Lett. **B278** (1992) 363;  
J. Bartels, A. De Roeck and M. Loewe, Z. Phys. **C54** (1992) 635.
- [6] E. Mirkes and D. Zeppenfeld, Phys. Lett. **B380** (1996) 205, [hep-ph/9511448].
- [7] W.T. Giele and E.W.N. Glover, Phys. Rev. D **46** (1992) 1980;  
W.T. Giele, E.W.N. Glover, and D.A. Kosower, Nucl. Phys. **B403** (1993) 633.
- [8] M. Glück, E. Reya and A. Vogt, Z. Phys. **C67** (1995) 433.
- [9] H. Plochow-Besch, Int. J. Mod. Phys. **A10** (1995) 2901.
- [10] E. Mirkes and D. Zeppenfeld, In the proceedings of “QCD and QED in Higher Orders” 1996 Zeuthen Workshop on Elementary Particle Theory, April 22-26, 1996 [hep-ph/9606332].
- [11] The cuts are similar to the ones used in the present H1 forward jet analysis. We thank A. De Roeck and E.M. Mroczko for this information.

[12] H1 Collaboration, S. Aid et al., Phys. Lett. **B356** (1995) 118.

[13] J. Bartels, V. Del Duca, A. De Roeck, D. Graudenz, and M. Wüsthoff, preprint DESY-96-036 (1996), [hep-ph/9604272].